CONSTRAINTS ON THE INTERSTELLAR DUST FLUX BASED ON STARDUST@HOME SEARCH RESULTS. A. J. Westphal, C. Allen, D. Anderson, S. Bajt, H. A. Bechtel, J. Borg, F. Brenker, J. Bridges, D. E. Brownlee, M. Burchell, M. Burghammer, A. L. Butterworth, P. Cloetens, A. M. Davis, C. Floss, G. J. Flynn, D. Frank, Z. Gainsforth, E. Grün, P. R. Heck, J. K. Hillier, P. Hoppe, L. Howard, G. R. Huss, J. Huth, A. Kearsley, A. J. King, B. Lai, J. Leitner, L. Lemelle, H. Leroux, R. Lettieri, P. Lyverse, W. Marchant, L. R. Nittler, R. C. Ogliore, F. Postberg, M. C. Price, S. A. Sandford, J. A. Sans Tresseras, S. Schmitz, T. Schoonjans, G. Silversmit, A. Simionovici, R. Srama, F. J. Stadermann, T. Stephan, J. Stodolna, R. M. Stroud, S. R. Sutton, R. Toucoulou, M. Trieloff, P. Tsou, A. Tsuchiyama, T. Tyliczszak, B. Vekemans, L. Vincze, J. Von Korff, D. Zevin, M. E. Zolensky, >29,000 Stardust@home dusters, *Affiliations are given at http://www.ssl.berkeley.edu/∼westphal/ISPE/.*

Recent advances in active particle selection in the Heidelberg Van der Graaf (VdG) dust accelerator have led to high-fidelity, low-background calibrations of track sizes in aerogel as a function of particle size and velocity in the difficult regime above 10 km sec^{-1} and submicron sizes [1]. To the extent that the VdG shots are analogs for interstellar dust (ISD) impacts, these new measurements enable us to place preliminary constraints on the ISD flux based on Stardust@home data.

Sample collection: The Stardust interstellar collector, comprising aerogel tiles and aluminum foils, was exposed for two periods to the interstellar dust stream in 2000 and 2002 for a total of 229 days [2]. The heliocentric distance of the spacecraft was 1.6-2.2 AU during the first exposure, and 1.6-2.7 AU for the second exposure. With the exception of 34 days during the second collection period, the collector tracked the interstellar dust stream, assumed to originate from ecliptic latitude $+2.5^\circ$, ecliptic longitude 252°, for particles with $\beta = 1$. Here β is the dimensionless ratio of force due to radiation pressure in sunlight to gravitational force. The spacecraft attitude was nominally maintained in a deadband of $\pm 15^\circ$.

Image data collection: We used an automated microscope to collect digital imagery of aerogel tiles in the Stardust Interstellar Collector. The field of view was 480 μm × 360 μm, and the spatial resolution was 0.47 μm pixel^{-1}. In each field of view, the scanning system collected a QuickTime movie, called a "focus movie", consisting of ∼43 frames acquired during a slow slew of the microscope's vertical axis through 200μm. During Phase I and Phase II of this project, we collected ∼ 200 000 focus movies.

Stardust@home: We searched for candidate interstellar dust impacts in the image data using a massively-distributed, internet-based virtual microscope (VM) that we called Stardust@home (S@h)[3]. Here we report on the results from Phases I and II of S@h. We prepared the raw focus movies for internet-based searching by splitting them into individual frames, and compressing each frame in jpeg format. After the processing, we uploaded the image data to the Amazon S3 "cloud". These images were then available for downloading to the VM as described below. Through one of the online forums on the Stardust@home website, Stardust@home volunteers named themselves "dusters". We adopt the same nomenclature here. To qualify to participate, a potential volunteer first had to go through a training and testing on the Stardust@home website. Over Phases I and II of Stardust@home, 28 573 people passed the test and registered as S@h dusters.

Focus movies were chosen randomly by the VM server. Dusters responded to each focus movie by clicking on the location of the deepest visible feature in the candidate track; pressing a "no track" button if no candidate was found; or pressing a "bad focus" button if no surface could be identified, or if the topography within the field of view prevented an adequate search.

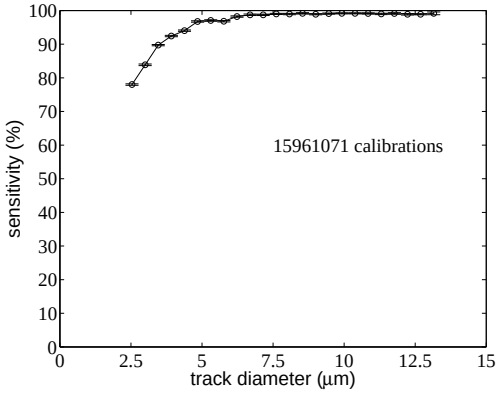

Figure 1: Detection efficiency for calibration movies during S@h Phases I and II, based on 1.6×10^7 responses.

We measured detection efficiencies and rate of false positives (the equivalent of noise rate in an electronic detector) using images with known characteristics – so-called calibration movies. Half of the calibration movies were focus movies from the Stardust Interstellar dataset into which the image of a 12μm diameter track was dubbed. The track was produced by the impact of a > 10 km sec^{-1} carbonyl Fe particle at the Heidelberg VdG dust accelerator, in an aerogel tile similar to the Stardust tiles. We used this track as a calibrant because it was the best option available, but its fidelity as an analog to real interstellar dust impacts was somewhat uncertain because of large background of apparently slow particles. The fidelity of this track was confirmed recently by recent experiments at Heidelberg using a dramatically improved electronic filter[1]. The track image was randomly rotated through 2π and scaled in diameter and independently in depth. The scale factor in diameter was chosen randomly in the range 0.2 to 2.0. The other half of the calibration movies were focus movies from the Stardust Interstellar dataset which we had carefully examined and determined to be blank. For Phase I and Phase II we used 2 421 and 3 021 calibration focus movies, respectively. In Phase II we used two different candidate tracks as calibrations, one of which was identical the one used in Phase I, the other was an unresolvable linear "whisker" feature in the aerogel. Any given search had a 20% probability of being a calibration movie. The dusters knew in general of the existence of

calibration movies, but the VM presented no information that would allow a duster to know whether any specific movie was a calibration movie or not.

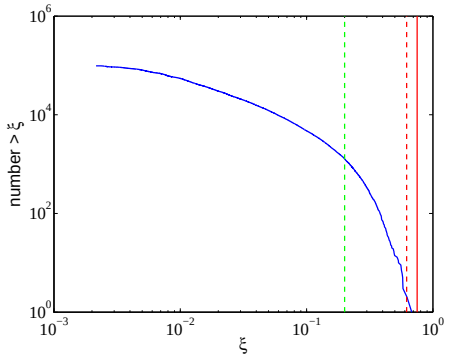

Figure 2: Integral distribution of the trigger fraction ξ over all movies with search multiplicity > 50.

The use of calibration movies had two serendipitous advantages. First, we used the responses to calibration movies to automatically generate an individual, real-time score for each duster, consisting of the number of correct responses to calibration movies less the number of incorrect responses. Also, the frequent presentation of calibration images helps to maintain attention in lengthy searches for rare events.

In Fig. 1 we show the ensemble wide detection efficiency ("sensitivity") for combined phases I and II, based on 16 million responses to calibration movies. The sensitivity spectra for individual phases are similar to that of the combined phases. The ensemble-wide false positive rate, equivalent to noise rate in an electronic detector, for Phase I and II was 0.5% in both phases. The minimum ensemble-wide detection efficiency was ~ 0.75, at the smallest track diameter, 2.5μm.

For each field of view, we define a trigger fraction ξ, which is the fraction of positive responses among all searches. In Fig. 2 we show the integral distribution of ξ, for fields of view which have been searched at least 50 times. The median search multiplicity in this dataset was 181. In the figure, we indicate the minimum expected value of ξ for genuine tracks in the limit of infinite search multiplicity, $\xi = 0.75$. However, because the search multiplicity was finite, statistical fluctuations cause a dispersion in ξ. We indicate with the dashed red line the approximate 2σ one-sided lower limit $\xi \sim 0.62$ for genuine tracks. The Berkeley team searched all 1260 fields of view with $\xi \geq 0.2$ and found no high-velocity track candidates in this range. These fields of view, taking into account overlaps, covered 216 cm^2 of aerogel collector area.

Results: In order to translate this null result into meaningful upper limits on the integral flux of high-velocity interstellar dust particles, we require a measured or theoretical dependence of track diameter on particle diameter, density and speed, and some informed assumptions about particle density and β. We have recently performed high-velocity calibration experiments using $0.25 - 0.35\mu$m diameter orthopyroxene, and $\sim 0.35\mu$m diameter polystyrene projectiles at speeds in the range 10-20 km sec^{-1}. Past experiments were ambiguous because of large backgrounds of low velocity particles, but a new electronics selection unit has dramatically reduced the background level so that high-velocity particles can be distinguished. We find that the data can be fit to within $\sim 20\%$ with a model of the form $d_t = (k_d v_{15} + 1) d_p$ where d_t is the track diameter, d_p is the particle diameter, v_{15} is the collection speed in units of 15 km sec^{-1}. We find that $k_d \sim 18$ for orthopyroxene and $k_d \sim 12$ for polystyrene.

The impacting velocity of particles depends strongly on the value of β. Zero observed events gives a 2σ one-sided upper limit of 3.8 events [4]. In Fig. 3 we show the upper limits on the integral flux of high-velocity interstellar dust particles, for different choices of impacting velocity. The slight upturn in the limits at small particle sizes is due to the effect of decreasing sensitivity there.

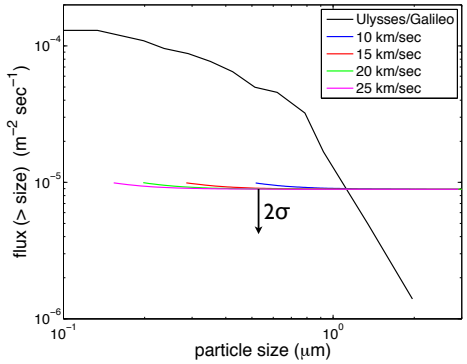

Figure 3: 2σ upper limits for different choices of impacting velocity. We also compare to measurements from the dust detectors onboard the Ulysses and Galileo spacecraft [5], taken at mean heliocentric distances of 4.2 AU and 4.5 AU, respectively.

Among 54 aerogel tracks in the Stardust Interstellar collector, we have identified four interstellar dust candidates, discussed in a companion abstract [6]. Two of these, tracks 30 and 34, were identified during Phases I and II of Stardust@home based on trajectories consistent with an origin in the IS dust stream and a composition inconsistent with spacecraft secondary ejecta. Based on a comparison of track morphology with the new laboratory calibration data, these now appear to be relatively low speed (< 10 km sec^{-1}) impacts, so are not included in the limits in Fig. 3. S@h phase I/II detection efficiency for low-speed tracks is not well-characterized because we did not use low-speed tracks calibration imagery there. The other two tracks were discovered during S@h phase III, which uses only low-speed calibration imagery, so these results cannot be integrated with phase I and II results. More work is needed in particle transport calculations and laboratory simulations before the apparent low-speed impacts can ruled in or out as interstellar dust candidates based on track morphology.

References: [1] Postberg F *et al.* (2011) 42nd LPSC, these proceedings. [2] Tsou, P., *et al.* (2003) JGR 108, 8113. [3] Westphal A. *et al.* (2006) 37th LPSC, 2225. [4] Gehrels N. (1986) ApJ *303*, 336. [5] Landgraf M. (1999) JGR *A105*, 10343. [6] Westphal A *et al.* (2011) 42nd LPSC, these proceedings.